





ASSESSING THE IMPACT OF METHODOLOGICAL DIFFERENCES ON GEOID MODEL PERFORMANCE

Kosasih PRIJATNA^{1}*, *Rahayu LESTARI¹*, *Brian BRAMANTO¹*,
Arisauna Maulidyan PAHLEVI², *Dudy D. WIJAYA¹*

DOI: 10.21163/GT_2024.192.10

ABSTRACT

The geoid serves as a critical reference surface for precise mapping applications, particularly in the context of satellite-based positioning systems like the Global Navigation Satellite System (GNSS). While GNSS offers efficient positioning solutions, it relies on an ellipsoidal surface that lacks physical meaning for vertical reference, highlighting the need for accurate geoid height models. A precise geoid model is essential for converting geodetic heights into orthometric heights, which are crucial for practical applications. This study investigates potential discrepancies among geoid models derived from different methods, focusing on the Stokes-Helmert (SH), remove-compute-restore (RCR), and *Kungl Tekniska Högskolan* (KTH) methods. The primary differences among these methods lie in their approaches to modifying the Stokes formula and their reduction schemes. Conducted in the central part of Java Island, Indonesia, this study uses terrestrial gravity observations to model the geoid and GNSS/leveling data for validating the geoid models. The RCR method demonstrated the highest accuracy, with an RMS error of 8.4 cm, outperforming the KTH method (9.2 cm) and the SH method (10.7 cm). Discrepancies between SH and RCR models were less pronounced, with differences around 30 cm, compared to over 1 meter between KTH and the other methods. The comparison with the global EGM2008 model showed that the gravimetric geoid models were more accurate, with RMS differences reaching up to 10 cm, primarily due to systematic differences with the EGM2008 model. Statistical analysis using t-tests with 95% confidence intervals indicated that the differences among SH, RCR, and KTH methodologies were not statistically significant. Despite the RCR method's apparent superior performance, these differences did not achieve statistical significance. The study notes the limitations of using a relatively limited terrestrial gravity dataset and emphasizes the need for incorporating additional gravity data, such as recent airborne gravity datasets, to improve geoid model performance. Future research should also aim for denser GNSS/leveling observations with stricter measurement requirements to provide a more robust absolute assessment of gravimetric geoid models.

Key-words: *geoid, Stokes-Helmert, remove-compute-restore, KTH.*

1. INTRODUCTION

Geoid is an equipotential surface, that best approximates the mean sea level in the ocean under an ideal condition and mainly serves as a vertical reference system (Sideris, 2021). The availability of a precise geoid height (undulation) model, defining the deviation between the geoid and ellipsoidal surfaces is important in precise mapping applications, particularly in the era of satellite-based positioning systems, i.e. using Global Navigation Satellite System (GNSS). The accuracy of instantaneous position estimates from GNSS observations reaches several centimeters (Gumilar et al., 2023; Krzyżek & Kudryś, 2022). Therefore, GNSS helps users to improve the productivity of large-scale maps compared when using conventional terrestrial methods, such as mapping using a total station as it provides positioning estimates in real-time and requires less labor (Kizil & Tisor, 2011).

¹*Geodetic Science, Engineering, and Innovation Research Group, Faculty of Earth Sciences and Technology, Institut Teknologi Bandung, 40132 Bandung, Indonesia; prijatna@itb.ac.id, rlestari2001@gmail.com, brian.bramanto@itb.ac.id, dudy.wijaya@itb.ac.id*

²*Directorate for Geospatial Reference System, Geospatial Information Agency of Indonesia (BIG), 16911 Cibinong, Indonesia; arisauna.maulidyan@big.go.id.*

**Corresponding author: prijatna@itb.ac.id*

Although GNSS offers efficient yet accurate positioning solutions, it also comes with a major drawback. The height estimate from GNSS position solutions is defined at the geodetic height system, i.e., using ellipsoidal surface as the vertical reference surface. Ellipsoidal surface is a simplified mathematical approximation of the geoid (Hofmann-Wellenhof et al., 2008). Consequently, the positioning estimates from GNSS observations do not have any physical meaning, i.e., cannot be used for determining the flow water direction. Therefore, to obtain physical height estimates (orthometric height) on the Earth surface using GNSS observations, the information related to the geoid height must be available accurately. Specifically for future large-scale mapping applications, it is essential to have a geoid model with high accuracy.

Having geodetic height estimates from GNSS observations and precise geoid height model, one can easily convert the geodetic height into orthometric height using the following equation:

$$H = h - N \quad (1)$$

where H is the orthometric height or the height difference between the geoid surface and the point on the Earth's surface, h is the geodetic height, defining the height on the Earth's surface referring to the ellipsoidal surface, and N is the geoid height undulating between the geoid and ellipsoid surfaces. It should be noted that geoid height can be positive or negative. It is positive when geoid surface lies above the ellipsoidal surface and vice versa. In simple, the relationship between Earth's topography, ellipsoidal and geoid surfaces is shown in **Fig. 1**.

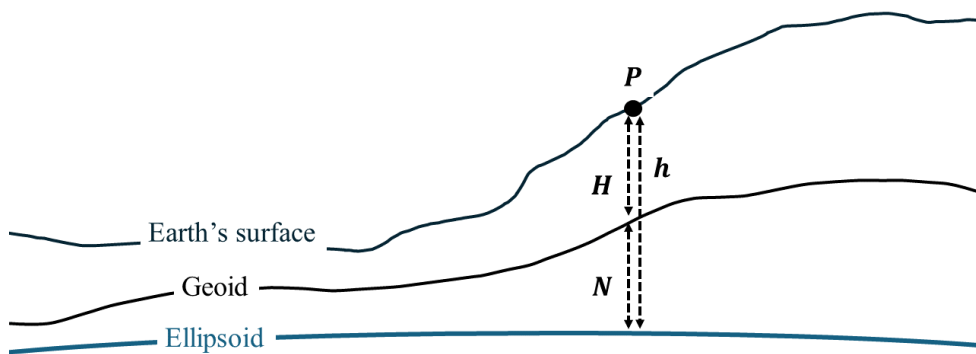


Fig. 1. A simplified diagram showing the relationship among the ellipsoid, geoid, and surface of the Earth.

The geoid height can be modeled based on geometric and gravimetric approaches. The geoid height modeled using the geometric approach relies on the combination of GNSS and leveling observations, providing heights that refer to ellipsoid and geoid surfaces. In principle, the geoid height can be then derived by calculating the difference between geodetic height from GNSS observation and orthometric height from leveling observation. While it seems that the computation of geometric geoid height is simple, the measurement is much more challenging and time-consuming (Erol & Erol, 2021). Therefore, the gravimetric approach is preferable as the technical aspects, e.g., measurement, are much more undemanding but a comprehensive understanding of gravimetric geoid height modeling is needed.

To model the geoid, there are many methods available such as the Stokes-Helmert (SH; Abbak et al., 2024; Ellmann & Vaníček, 2007; Lestari et al., 2023; Vaníček et al., 2013), Remove-Compute-Restore (RCR; Schwarz et al., 1990; Wu et al., 2020; Yildiz et al., 2012a), and *Kungl Tekniska Högskolan* (KTH; Sjöberg, 2003, 2020) methods. Each method has its own computational methodology, including procedures for handling terrain effects, mathematical models to continue gravity data and terrain effects, etc. Consequently, the geoid height estimates might vary depending on the selection of the methodology used regardless of the same gravity data used.

Consequently, ongoing research is crucial to develop a geoid model that achieves superior accuracy tailored to the specific conditions of our region, Indonesia, which includes varying topography with archipelagic situations. The three methods employed for comparison SH, RCR, and KTH represent the best practices currently available. Continued evaluation and refinement of these methods will be necessary to address the unique challenges posed by our geographic conditions and ensure the highest quality geoid modeling. Therefore, this paper aims to assess the geoid height estimates from different methods, i.e., the SH, RCR, and KTH methods, and investigates whether a significant discrepancy exists among the derived geoid models. For this purpose, we selected the central part of Java Island, Indonesia, as our test case as the relatively dense terrestrial gravity observations are available. In addition, GNSS/leveling observations that can be used to validate the resulting geoid height model are also available.

The remainder of this paper is described as follows: Section 2 describes the methodologies and data used to compute the geoid height model, Section 3 presents the results and discusses the findings, and finally, Section 4 presents the conclusion of the study and provides the direction for future research.

2. METHODS AND DATA

2.1. Stokes - Helmert Method

The Stokes-Helmert method is a method for geoid modeling that utilizes Stokes's Integral to convert gravity anomaly into geoid height, while Helmert's 2nd condensation serves as the reduction scheme. The calculation of geoid height using the Stokes method requires integration over the entire Earth with continuous gravity anomalies. The disturbing potential must obey to the Laplace equation above the geoid, ensuring that there is no mass above the surface where the gravity anomaly is situated (Hoffman-Wellenhof & Moritz, 2006; Jekeli et al., 2013). However, since gravity measurements using gravimeters are typically limited to the study area, the computations need to be supplemented with a lower-degree gravity field, such as the global geopotential model (GGM; Hoffman-Wellenhof & Moritz, 2006). The formula for calculating residual geoid height can be expressed as follows (Abbak et al., 2012):

$$N_{\Delta g} = \frac{R}{4\pi\gamma} \iint_{\sigma} \Delta g_{red} S(\psi) d\sigma \quad (2)$$

where N is the geoid height, Δg_{red} is the reduced Faye gravity anomaly that is defined as $\Delta g_{red} = \Delta g_{FA} - \Delta g_{GGM} - \Delta g_H$, with Δg_{FA} is the free-air gravity anomaly, Δg_{GGM} is the long-wavelength component from GGM, and Δg_H is the topographic gravity effect, γ is normal gravity, R is the mean of Earth's radius, and $S(\psi)$ is the Stokes' kernel can be written as:

$$S(\psi) = \sum_{n=2}^{\infty} \frac{2n+1}{n-1} P_n(\cos \psi) \quad (3)$$

where ψ is spherical distances between data points and computation points, $P_n(\cos \psi)$ is Legendre function, and n is degree.

The Helmert's 2nd condensation reduction scheme serves as a method to satisfy the requirements of Stokes's formula, which mandates the absence of masses above the geoid, and that the gravity anomaly must be referenced to the geoid (Heck, 2003a). This reduction involves several steps, initially, it involves calculating the direct topographical effect on gravity to replace the impact of surface masses on gravity with the effect of the mass layer on the geoid (Heiskanen & Moritz, 1967; Sideris & Forsberg, 1991; Vanicek & Kleusberg, 1987). Then, a downward continuation is applied to determine the gravity anomaly at the geoid by estimating the actual gravity anomaly at the geoid from

observation at the Earth's surface. Stokes' formula is then applied to the gravity anomalies at co-geoid. Finally, the computation of the indirect topographical effect is performed to complete the final geoid model, yields (Martinec et al., 1993):

$$N = N_{GGM} + N_{\Delta g_{red}} + N_{ind} \quad (4)$$

where N_{GGM} is the long-wavelength geoid contribution from GGM and N_{ind} is the indirect effect on the geoid height for Helmert's 2nd condensation.

2.2. RCR Method

The Remove-Compute-Restore (RCR) method, like the Stokes-Helmert method, uses Stokes' Integral but with a different reduction scheme. In this method, the computation involves the use of a quasigeoid for the approximation surface, which is done by using the RTM reduction scheme. The RCR method is commonly used in regional gravimetric geoid modeling, which aims to separate the long-, medium-, and short-wavelength geoid/gravity components (Schwarz et al., 1987, 1990; Sideris, 2013). Geoid modeling, when using the RCR technique, focuses on residual gravity anomaly data to streamline the calculation process (Hoffman-Wellenhof & Moritz, 2006). During the removal stage, the long-wavelength components (as derived from the global model) and short-wavelengths (as computed from the topographic model) are removed from the gravity data. Subsequently, in the computation stage, the band-pass filtered gravity anomalies are converted into either quasigeoid height or height anomaly using Stokes' formula. Once the computational stage is completed, the long-wavelengths and short-wavelengths are restored to obtain the complete quasigeoid height (Yildiz et al., 2012b). **Fig. 2** illustrates the contribution of each component: long-wavelengths (from the global model), medium-wavelengths (from gravity data), and short-wavelengths (from the topographic model).

In the RTM scheme, the reduction performed is not an isostatic topography reduction but produces anomalies similar to an isostatic topography anomaly. This scheme is often used for terrain reduction in quasigeoid modeling (Forsberg, 1984). This scheme involves the use of a reference surface (an average elevation surface) determined by introducing the low pass filter to the precise topographical model, obtaining a smoother elevation surface. This reduction technique requires the removal of the topographic mass above the reference surface and filling the mass below it (refer to **Fig. 3**; Bajracharya & Sideris, 2005; Yang et al., 2022).

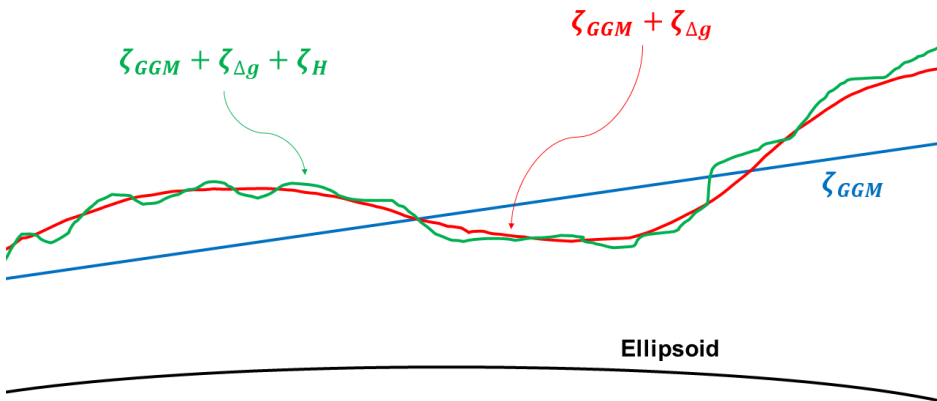


Fig. 2. Illustration of the contribution from various wavelength components to the quasigeoid height. ζ_{GGM} is the height anomaly of the long wavelength component, $\zeta_{\Delta g}$ is the height anomaly of the residual component, and ζ_H is the height anomaly of the short wavelength component.

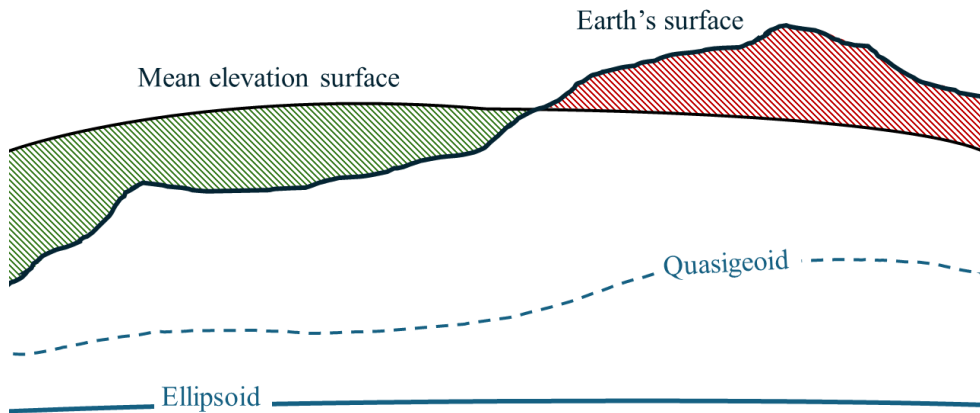


Fig. 3. An illustration showing the RTM configuration. The red-shaded area shows the region where more masses occur above the mean elevation surface, while the green-shaded area shows the region with a lack of masses below the mean elevation surface.

The method of utilizing geoid heights to depict the Earth's physical shape has a limitation: it necessitates knowledge of the mass density above the reference surface or requires certain assumptions to address this issue. To circumvent this limitation, an alternative approach is adopted, allowing for the formulation of the height anomaly as follows (Vu et al., 2019):

$$\zeta = \zeta_{GGM} + \frac{R}{4\pi\gamma} \iint_{\sigma} \Delta g_{res} S(\psi) d\sigma + \zeta_{RTM} \quad (5)$$

where Δg_{res} is the residual gravity anomaly defined as $\Delta g_{res} = \Delta g_{FA} - \Delta g_{GGM} - \Delta g_{RTM}$, with Δg_{RTM} is the corresponding RTM gravity effect, ζ_{GGM} is the height anomaly from GGM, and ζ_{GGM} is the RTM height anomaly. The height anomaly values are subsequently transformed into geoid height values using a formula that we call quasigeoid to geoid separation (QGS), expressed as follows (Heiskanen & Moritz, 1967):

$$QGS = \zeta - N \approx -\frac{\Delta g_{BA}}{\gamma} H \quad (6)$$

where Δg_B is the Bouguer gravity anomaly, γ is normal gravity, and H is the orthometric height. The Bouguer gravity anomaly, using a Bouguer plate approximation, can be mathematically defined as:

$$\Delta g_{BA} = \Delta g_{FA} - 0.1119H. \quad (7)$$

2.3. KTH Method

The KTH method, developed by *Kungl Tekniska Hogskolan* or KTH Royal Institute of Technology, utilizes the Modification Stokes by Sjöberg's technique to calculate the approximation of geoid height. By taking advantage of the orthogonality of spherical harmonics over the sphere, this method's equation can be represented as, with two sets of modification parameters s_n and b_n (Sjöberg, 1984; Sjöberg, 1991, 2003):

$$\tilde{N} = \frac{R}{4\pi\gamma} \iint_{\sigma_0} S^L(\psi) \Delta g_{FA} d\sigma + \frac{R}{2\gamma} \sum_{n=2}^M b_n \Delta g_{GGM} \quad (8)$$

where $S^L(\psi)$ is the modified Stokes' function, L is the selected maximum degree of the arbitrary parameters s_n of the modification, and M is the upper limit of the GGM used. The modified Stokes' function can be formulated as:

$$S^L(\psi) = \sum_{n=2}^{\infty} \frac{2n+1}{n-1} P_n(\cos \psi) - \sum_{n=2}^L \frac{2n+1}{2} s_n P_n(\cos \psi) \quad (9)$$

Then, modification parameter s_n can be expressed by:

$$h_k = \sum_{n=2}^L a_{kn} s_n, \quad k = 2, 3, \dots, L \quad (10)$$

where h_k is the element of the observable vector and a_{kn} is the element of design matrix.

Furthermore, the KTH method incorporates several additive corrections: the combined topographic correction (δN_{comb}^{top}) represents the combined direct and indirect topographical effects on the geoid, the combined atmospheric correction (δN_{comb}^{atm}) accounts for the combined direct and indirect atmospheric effects, and the ellipsoidal correction (δN_{ell}) adjusts for the spherical approximation of the geoid in Stokes' formula to the ellipsoidal reference surface. Thus, the geoid height can be expressed as (Sjöberg, 2003):

$$N = \tilde{N} + \delta N_{comb}^{top} + \delta N_{comb}^{atm} + \delta N_{ell} \quad (11)$$

2.4. Validation

The resulting gravimetric geoid models will be further validated against the geometric geoid model derived from GNSS/leveling observations (see Eq. 1). This validation process is referred to as absolute validation, where the discrepancy between gravimetric and geometric geoids is being assessed. This discrepancy reads:

$$\Delta N = N^{gra} - N^{geo} \quad (12)$$

where N^{gra} is the gravimetric geoid and N^{geo} is the geometric geoid.

To thoroughly evaluate the effectiveness of a geoid model using GNSS/leveling data, a relative validation method is further employed. This involves calculating the differences between the differential geoid heights of both the gravimetric and geometric models across various baselines derived from GNSS/levelling benchmarks. These discrepancies are then expressed in relative terms, measured in m/km, reads (Abbak & Ustun, 2015):

$$\Delta N_{ij} = \frac{|(N_i^{gra} - N_j^{gra}) - (N_i^{geo} - N_j^{geo})|}{d_{ij}} \quad (13)$$

where ΔN_{ij} is relative value and d_{ij} is spherical distance from i to j .

2.5. Summary of Methodology for Each Method

The summary of the methodology of the Stokes-Helmert, RCR, and KTH methods is shown in **Fig. 4**. The variation between these three methods is mainly due to differences in their reduction schemes and how they handle the Stokes integration when transforming gravity values into geoid heights. The SH method employs co-geoid as an approximate surface for the geoid.

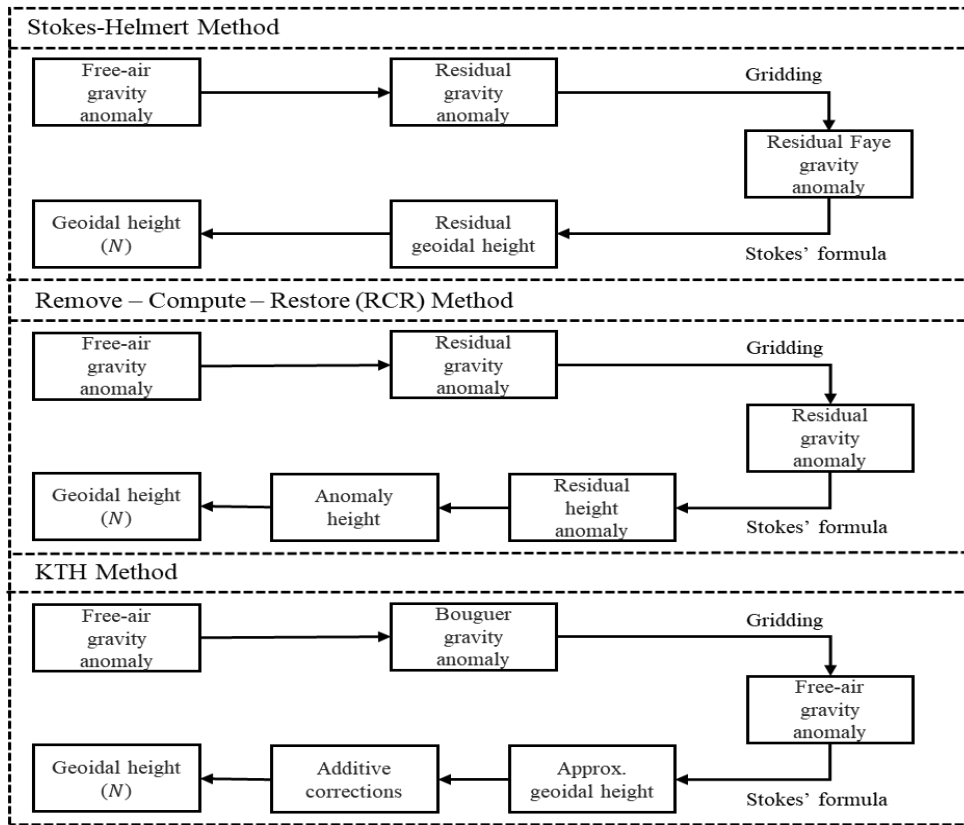


Fig. 4. Summary of the methodologies used in this study.

The reduction process utilizes 2nd Helmert’s Condensation involves redistributing mass back to the geoid itself. Topographic mass is reallocated based on the local condensation procedure, which involves compressing the topographic column onto the condensation surface (Heck, 2003b). Then, the RCR method calculates residual gravity anomalies by incorporating short-wavelengths topographical gravity effects from RTM scheme. Consequently, the estimates read as height anomalies instead of geoid height. Therefore, further calculations are required to convert the height anomaly values into geoid heights, as previously mentioned (Omang & Forsberg, 2000). Finally, the KTH method does not use any reduction scheme, the calculation is carried out directly on the topographic surface. Instead, an additive correction (see eq. 11) is applied after the geoid approximation value is obtained.

A key difference among the methods compared, particularly noticeable in the KTH method, lies in the modification of the Stokes kernel used for geoid calculations (see eq. 8 and eq. 9). For the case of SH and RCR methods, a slightly different Stokes’ modification is further introduced. Specifically, we applied the Wong-Gore modification to the Stokes function. The modified Stokes function for SH and RCR methods is defined as follows (Forsberg & Tscherning, 2008; Wong & Gore, 1969):

$$S_{mod}(\psi) = S(\psi) - \sum_{n=2}^M \alpha(n) \frac{2n+1}{n-1} P_n(\psi) \tag{14}$$

$$\alpha(n) = \begin{cases} 1 & \text{for } 2 \leq n \leq M_1 \\ \frac{M_2 - n}{M_2 - M_1} & \text{for } M_1 \leq n \leq M_2, \quad n = 2, \dots, M \\ 0 & \text{for } M_1 \geq n \leq M_2 \end{cases} \tag{15}$$

where M_1 and M_2 represent the lower and upper degree of spheroidal modification for the kernel integration. To obtain the appropriate spherical caps, M_1 , and M_2 , a trial-and-error evaluation is conducted to achieve the best results.

2.6. DATA

2.6.1. GNSS/Leveling

The GNSS/leveling data utilized in this study were surveyed and processed by the Geospatial Information Agency (Badan Informasi Geospasial, BIG) at 186 points, spanning from north to south between Semarang and Yogyakarta (refer to **Fig. 5c**). The GNSS observations were conducted using the relative differential method, tied to the nearby CORS (Continuously Operating Reference System) within the research area. Additionally, leveling was performed with respect to the tidal benchmark (BM) in the research area. The geoid heights derived from the GNSS/leveling measurements serve as validation values against the geoid model generated using the gravimetric method as described in Section 2.4.

2.6.2 Terrestrial Gravity Data

The terrestrial gravity data was gathered by BIG in 2019. A total of 264 data points were collected, covering the central area of Java Island that were mostly clustered in Semarang and Yogyakarta. These measurements were conducted at 5-kilometer intervals using the Scintrex CG-5 relative gravimeters (refer to **Fig. 5a**).

2.6.3. Digital Elevation Model

The Digital Elevation Model (DEM) serves as the short-wavelength component and is essential for computing terrain correction, indirect effect, and generating the residual terrain model (RTM). We utilized SRTM 1" (SRTM, 2015) data for land areas and SRTM 15"+ (Tozer et al., 2019) for oceanic regions (refer to **Fig. 5d**). These data were further combined and resampled to 1", obtaining a consistent grid resolution. To derive parameters from the RTM, we employed the TGF software (Yang et al., 2020). Otherwise, an in-house program package is used to calculate the remaining parameters.

2.6.4. Global Geopotential Model

To address the scarcity of terrestrial gravity data, we incorporated a global geopotential model (GGM) to fill the gaps and enhance the quality of the gravimetric geoid. Additionally, GGM includes a long-wavelength component as it requires integration across the entire Earth due to the use of Stokes' integral. Specifically, we utilized the Earth Gravitational Model 2008 (EGM2008) with degrees and orders of 2190, which is known to have a resolution of approximately 5 arc minutes or roughly 9.13 kilometers (Pavlis et al., 2012).

2.6.5. Fill-in Gravity Data

The process of calculating a local gravimetric geoid model involves integrating terrestrial gravity data within a specific area. To ensure accuracy and precision, it's essential to address any gaps in gravity information by incorporating data from alternative sources (Matsuo & Kuroishi, 2020). In this study, we added the gravity data by combining EGM2008 with a degree and order of 2190 and RTM obtained from SRTM 1" for land areas, and SRTM 15"+ for oceanic regions (refer to **Fig. 5b**).

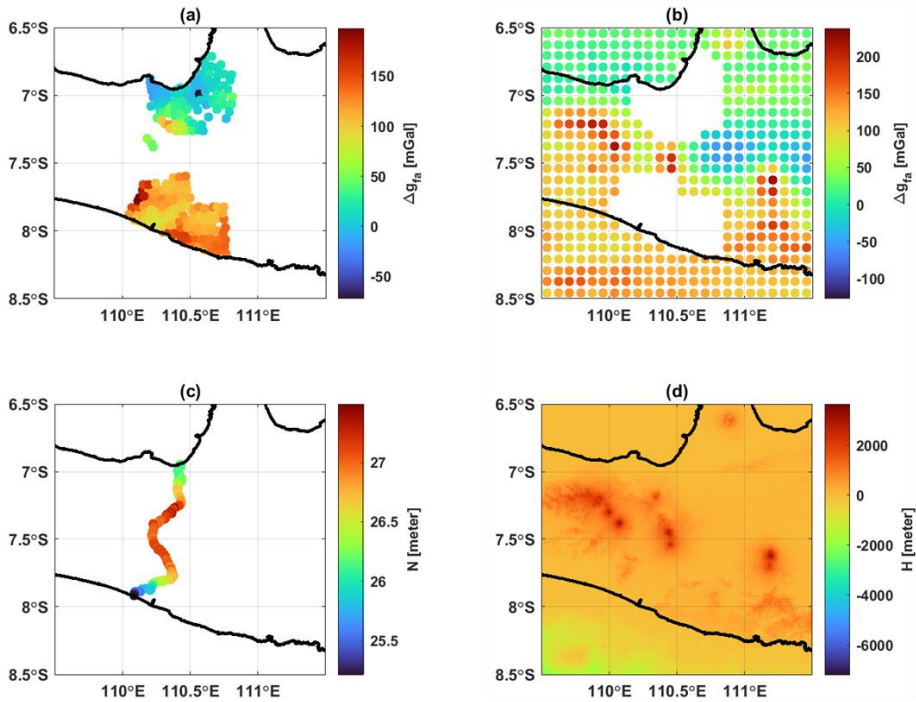


Fig. 5. Free-air gravity anomalies from terrestrial gravity data (a) and fill-in gravity data (b). Panel (c) and (d) show the distribution of geoidal height from GNSS/leveling and topography from the combination between SRTM1” and SRTM15”+ models, respectively.

3. RESULT AND DISCUSSION

The investigation involved the computation of three local gravimeters model using different methodologies: Stokes-Helmert (SH), Remove-Compute-Restore (RCR), and *Kungl Tekniska Högskolan* (KTH). The primary differences among these methods lie in their reduction schemes and how they handle the computational aspects of the Stokes formula. The SH method uses a reduction scheme based on the co-geoid surface, while RCR operates on the quasigeoid. The KTH method directly utilizes the geoid surface. In terms of the Stokes formula, the SH and RCR methods adjust the gravity anomaly, whereas KTH modifies the Stokes kernel. Computationally, both SH and RCR employ the multiband spherical Fast Fourier Transform (FFT), while KTH uses ordinary numerical integration. Geoid modeling performed using the SH and RCR methods was based on in-house programs package, while the KTH method utilized the LSMSSOFT software (Abbak & Ustun, 2015).

Despite these differences, all three approaches share common procedures during computation, including utilizing spherical caps of 1.28° and the application of bias correction on the resulting geoid models. Bias correction was obtained by calculating the average difference between the gravimetric geoid model and validation data. The variations observed among the three geoid models (refer to **Fig. 6**) are relatively minor. However, regions with elevated topography exhibit more distinct color contrasts in the KTH model compared to the SH and RCR models. According to the statistical data (refer to **Table 1**), the average geoid height within the study area (110° - 111° E and 6.5° - 8° S) for the SH, RCR, and KTH methods are 26.620 m, 26.593 m, and 26.605 m, respectively, representing a difference of approximately 3 cm. When considering the highest and lowest geoid height values within the study area, both SH and RCR methods demonstrate similar ranges, spanning from 24.347 m to 28.836 m for SH and 24.323 m to 28.766 m for RCR. In contrast, the KTH method exhibits a notable disparity in the minimum geoid height value within the study area, differing by 40 cm compared to the other methods. The range of geoid model values utilizing the KTH method extends from 23.938 m to 28.816 m.

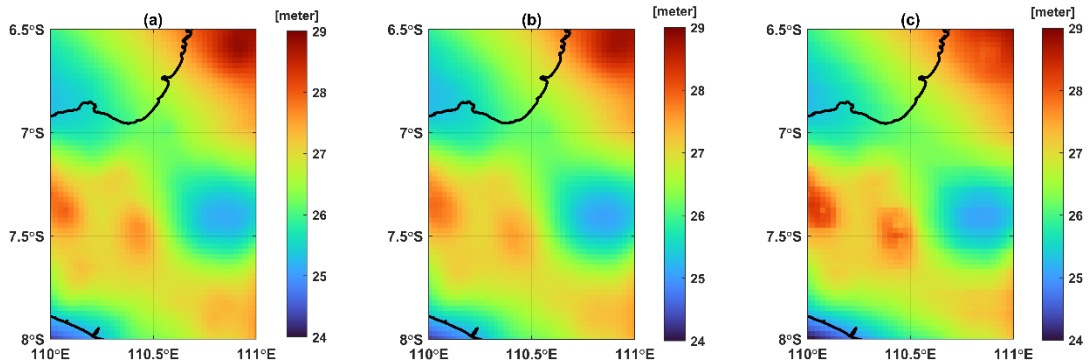


Fig. 6. Geoid models obtained when implementing SH (a), RCR (b), and KTH (c) methodologies.

Table 1.
Statistics of the geoid models when using different methodologies.

Geoid	Min [m]	Max[m]	Mean[m]
SH	24.347	28.836	26.620
RCR	24.323	28.766	26.593
KTH	23.938	28.816	26.605

Fig. 7 illustrates the discrepancies among each model, presenting the differences between the SH method and the RCR method (see **Fig. 7a**), between the SH method and the KTH method (**Fig. 7b**), and between the RCR model and the KTH model (**Fig. 7c**). The disparity between the SH and RCR models is relatively insignificant compared to the disparity between the KTH model and both the SH and RCR models. Particularly noticeable differences are observed between the KTH model and the other two models, notably in the northern and central mountainous regions, as well as in the southern areas. These variations are further elucidated by the statistical data presented in **Table 2**. The differences between the SH and RCR models range from -9.8 cm to 28.4 cm, while the disparity between the SH and KTH models spans from -4.5 cm to 70.8 cm. Similarly, the difference between the RCR and KTH models ranges from -47.2 cm to -62.9 cm. As previously outlined, the variation between the SH and RCR methods is relatively minor, with mean, root mean square (RMS), and standard deviation (STD) values of 2.7 cm, 4.4 cm, and 3.5 cm, respectively. In contrast, the disparity between the SH and KTH models yields mean, RMS, and STD values of 1.5 cm, 12.7 cm, and 12.7 cm, respectively. Meanwhile, the difference between the RCR and KTH models results in mean, RMS, and STD values of -1.2 cm, 11.7 cm, and 11.6 cm, respectively.

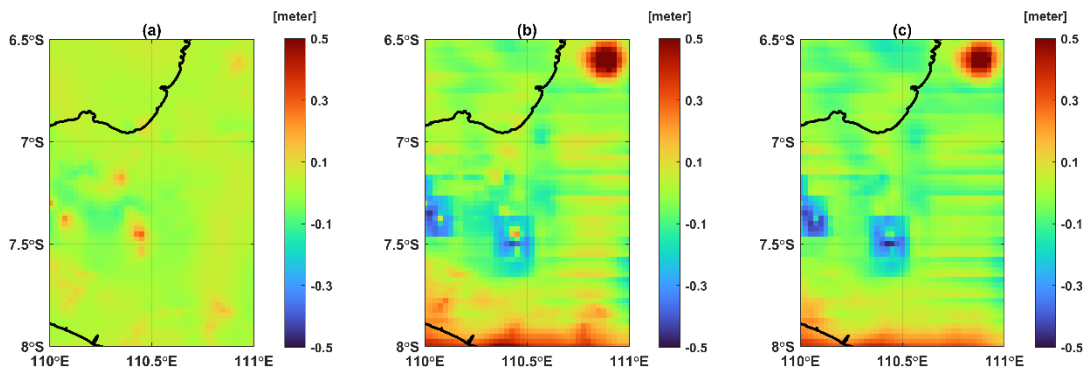


Fig. 7. Geoid differences between SH and RCR methods (a); SH and KTH methods (b); RCR and KTH methods (c).

Table 2
Statistics of the differences between the geoid models across different methodologies.

Geoid	Min [m]	Max [m]	Mean [m]	RMS [m]	STD [m]
SH – RCR	-0.098	0.284	0.027	0.044	0.035
SH – KTH	-0.451	0.708	0.015	0.127	0.127
RCR – KTH	-0.472	0.629	-0.012	0.117	0.116

Following the reduction of the geoid model by its bias value relative to the gravimetric geoid model produced by GNSS/leveling, validation procedures are undertaken. Notably, the shape of the geoid surface in the validation area exhibits minimal discrepancies (refer to **Fig. 8**). We also incorporated EGM2008 into the validation process to assess the extent to which the global model (EGM2008) deviates from our gravimetric model. Based on the values from the figure, it appears that the difference between the EGM2008 geoid model and our gravimetric model, when compared to the validation geoid, is primarily due to a significant shift of about 15 cm.

The three models demonstrate standard deviation and RMS differences of only approximately 1-2 cm (refer to **Table 3**), with the RCR method yielding the most favorable outcomes compared to the others. Specifically, the standard deviation and RMS values for the SH, RCR, KTH, and EGM2008 models are 10.7 cm, 8.4 cm, 9.2 cm, and 10.2 cm, respectively. This table shows that each model exhibits disparities with the validation data (GNSS/leveling), ranging from -50.2 cm to 25.3 cm for the SH method, -46.9 cm to 19 cm for the RCR method, -41.5 cm to 22.6 cm for the KTH method, and -66.5 cm to 3.7 cm for the EGM2008. In addition, the relative assessment demonstrates good overall precision of about 0.006 m/km or corresponds to an error of 6 mm for every one kilometer, making it suitable for most practical applications.

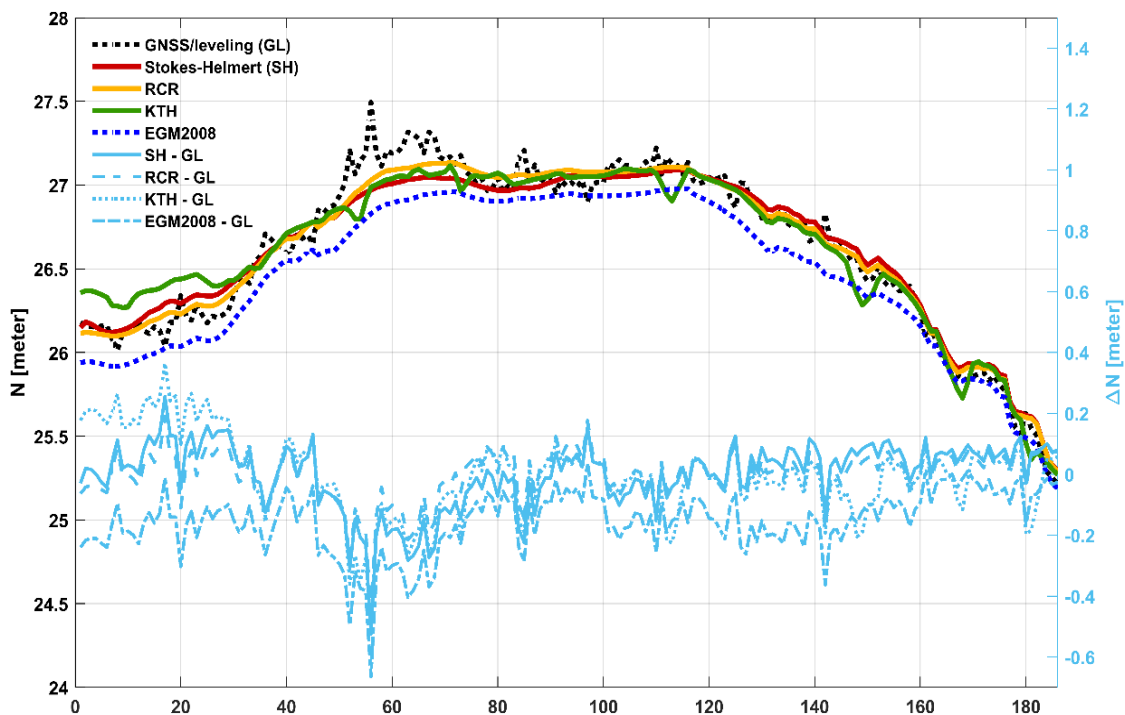


Fig. 8. The comparison between geometric and gravimetric geoid models. Light blue lines display the differences between geometric and gravimetric geoid models. Note the difference in scale.

Table 3

Statistics from the validation of the SH, RCR, and KTH method geoid models.

Geoid	Absolute assessment					Relative assessment		
	Min [m]	Max [m]	Mean [m]	RMS [m]	STD [m]	Min [m/km]	Max [m/km]	Mean [m/km]
SH	-0.521	0.253	0.000	0.107	0.107	0.000	1.390	0.006
RCR	-0.469	0.190	0.000	0.084	0.084	0.000	1.389	0.005
KTH	-0.415	0.226	0.000	0.092	0.092	0.000	1.409	0.007
EGM2008	-0.665	0.037	-0.156	0.186	0.102	0.000	1.399	0.006

Looking closer at **Fig. 8** and **Table 3**, the discrepancy between geometric and gravimetric geoid models seems to be prominent at several points of validation. This affects the corresponding maximum and minimum discrepancy in absolute and relative assessments. Particularly for the absolute assessment, the absolute minimum discrepancy is larger than twice the standard deviation value (corresponds to 95% confidence intervals). At the same time, the maximum values for the relative assessment are significantly different compared to the mean values. This highlights possible outliers that are likely due to the errors in GNSS/leveling measurements. Lestari et al. (2023) stated that the leveling measurements underwent relatively strict measurement requirements, including the difference of height difference between forward and backward leveling was less than $8\sqrt{K}$ mm, with K being the distance of the leveling section in kilometer units. Hence, another possible error is likely caused by the GNSS measurements. The GNSS observations were set up using tripods, making it prone to error in measuring the height of the antenna.

In this study, modeling the geoid using RCR methodology seems to be better than those other methodologies, including the SH and KTH methods. Hence, we further conducted a statistical analysis to investigate whether the accuracy performance across methodologies is statistically significant or not, using a t-test analysis with 95% confidence intervals based on the results of the absolute assessment. The t-values across the geoid models computed in this study fell below the critical t-value, suggesting that the differences in geoid models generated by the SH, RCR, and KTH methodologies are not statistically significant despite the apparent superiority of the RCR method. This finding is consistent with previous research conducted by, e.g., Wang et al. (2021), which also observed minimal differences in the results of geoid models derived from various methodologies made by different agencies using a similar dataset. This further supports the robustness of different geoid modeling techniques.

4. CONCLUSIONS

Geoid modeling was conducted for the central part of Java Island using terrestrial gravity data and three different methodologies: Stokes-Helmert (SH), Remove-Compute-Restore (RCR), and KTH. The primary differences among these methods are in their approaches to the Stokes formula and reduction scheme. Among the methods, the RCR method emerged as the most effective in terms of geoid model accuracy, with an RMS of 8.4 cm, outperforming the KTH method at 9.2 cm and the SH method at 10.7 cm. At the same time, the discrepancies in the geoid surface between the SH and RCR methods were less pronounced compared to those observed with the KTH method. This is evident from the range of difference values generated, where the disparity between the surfaces of the SH and RCR method models spans around 30 cm, while the difference between the KTH method and both the SH and RCR methods exceeds 1 meter. Further comparison with the global model of EGM2008 indicates that the resulting gravimetric geoid models are better with the difference in RMS reaches up to 10 cm. This discrepancy is primarily due to a systematic difference between the EGM2008 geoid model and our gravimetric geoid models.

Given the observed differences in geoid models, we conducted a t-test analysis with 95% confidence intervals to determine if these differences were statistically significant. The results revealed that the t-values were below the critical threshold, implying that the variations between the

SH, RCR, and KTH methodologies are not statistically significant. Despite the RCR method demonstrating apparent superior performance, these differences do not reach statistical significance.

We stress that this study is made with a relatively limited gravity dataset, where only terrestrial gravity dataset is used. Future studies should be incorporating more gravity datasets, e.g., recent airborne gravity dataset (Bramanto et al., 2021), covering the gaps in in-situ gravity observations. This effort could potentially improve the performance of geoid models as suggested by Bjelotomić Oršulić et al., (2020). In addition, we acknowledge that only one profile line of GNSS/leveling observations is available, making it challenging to make a robust external absolute assessment of the resulting gravimetric geoid models. Denser GNSS/leveling observations with stricter measurement requirements are essential for future work.

ACKNOWLEDGEMENT

We would like to thank the data support provided by the Directorate for Geospatial Reference System, Geospatial Information Agency of Indonesia. Three anonymous reviewers and the editor are greatly acknowledged for their constructive comments that significantly enhanced the quality of the manuscript.

This study was funded by Penelitian, Pengabdian Masyarakat, dan Inovasi (PPMI) Program of Faculty of Earth Sciences and Technology (FITB), Institut Teknologi Bandung.

REFERENCES

- Abbak, R. A., Erol, B., & Ustun, A. (2012). Comparison of the KTH and remove-compute-restore techniques to geoid modelling in a mountainous area. *Computers and Geosciences*, 48, 31–40. <https://doi.org/10.1016/j.cageo.2012.05.019>
- Abbak, R. A., Goyal, R., & Ustun, A. (2024). A user-friendly software package for modelling gravimetric geoid by the classical Stokes-Helmert method. *Earth Sci. Inform.* <https://doi.org/10.1007/s12145-024-01328-0>
- Abbak, R. A., & Ustun, A. (2015). A software package for computing a regional gravimetric geoid model by the KTH method. *Earth Science Informatics*, 8(1), 255–265. <https://doi.org/10.1007/s12145-014-0149-3>
- Bajracharya, S., & Sideris, M. G. (2005). *Terrain-aliasing effects on gravimetric geoid determination*. 54(I), 3–16.
- Bjelotomić Oršulić, O., Markovinić, D., Varga, M., & Bašić, T. (2020). The impact of terrestrial gravity data density on geoid accuracy: case study Bilogora in Croatia. *Survey Review*, 52(373), 299–308. <https://doi.org/10.1080/00396265.2018.1562747>
- Borghi, A., Barzaghi, R., Al-Bayari, O., & Al Madani, S. (2020). Centimeter precision geoid model for Jeddah region (Saudi Arabia). *Remote Sensing*, 12(12). <https://doi.org/10.3390/RS12122066>
- Bramanto, B., Prijatna, K., Pahlevi, A. M., Sarsito, D. A., Dahrin, D., Variandy, E. D., & Munthaha, R. I. S. (2021). Determination of gravity anomalies in Java, Indonesia, from airborne gravity survey. *Terr. Atmospheric Ocean. Sci.*, 32(5.2). <https://doi.org/10.3319/TAO.2021.06.04.01>
- Ellmann, A., & Vaniček, P. (2007). UNB application of Stokes-Helmert's approach to geoid computation. *Journal of Geodynamics*, 43(2), 200–213. <https://doi.org/10.1016/j.jog.2006.09.019>
- Erol, S., & Erol, B. (2021). A comparative assessment of different interpolation algorithms for prediction of GNSS/levelling geoid surface using scattered control data. *Measurement*, 173, 108623. <https://doi.org/10.1016/j.measurement.2020.108623>
- Forsberg, R. (1984). A study of terrain reductions, density anomalies and geophysical inversion methods in gravity field modelling (No. OSU/DGSS-355). Ohio State Univ Columbus Dept of Geodetic Science and Surveying. In *Ohio State Univ Columbus Dept of Geodetic Science and Surveying*.

- Forsberg, R., & Tscherning, C. C. (2008). *An overview manual for the GRAVSOF: Geodetic Gravity Field Modelling Programs* (Issue August).
- Gumilar, I., Fauzan, S. A., Bramanto, B., Abidin, H. Z., Sugito, N. T., Hernandi, A., & Handayani, A. P. (2023). The benefits of multi-constellation GNSS for cadastral positioning applications in harsh environments. *Appl. Geomat.*, *15*(4), 975–989. <https://doi.org/10.1007/s12518-023-00525-8>
- Heck, B. (2003a). On Helmert's methods of condensation. *Journal of Geodesy*, *77*(3), 155–170. <https://doi.org/10.1007/s00190-003-0318-5>
- Heck, B. (2003b). On Helmert's methods of condensation. *Journal of Geodesy*, *77*(3), 155–170. <https://doi.org/10.1007/s00190-003-0318-5>
- Heiskanen, W. A., & Moritz, H. (1967). *Physical Geodesy*. Freeman.
- Hoffman-Wellenhof, B., & Moritz, H. (2006). *Physical Geodesy (Second, corrected edition)*. SpringerWienNewYork. <https://doi.org/10.1007/978-3-211-33545-1>
- Hofmann-Wellenof, B., Lichtenegger, H., & Wasle, E. (2008). *GNSS – Global Navigation Satellite Systems: GPS, GLONASS, Galileo, and more*. Springer-Verlag.
- Jekeli, C., Yang, H. J., & Kwon, J. H. (2013). Geoid determination in South Korea from a combination of terrestrial and airborne gravity anomaly data. *Journal of the Korean Society of Surveying Geodesy Photogrammetry and Cartography*, *31*(6 PART 2), 567–576. <https://doi.org/10.7848/ksGPC.2013.31.6-2.567>
- Kizil, U., & Tisor, L. (2011). Evaluation of RTK-GPS and Total Station for applications in land surveying. *J. Earth Syst. Sci.*, *120*(2), 215–221. <https://doi.org/10.1007/s12040-011-0044-y>
- Krzyżek, R., & Kudrys, J. (2022). Accuracy of GNSS RTK/NRTK height difference measurement. *Appl. Geomat.*, *14*(3), 491–499. <https://doi.org/10.1007/s12518-022-00450-2>
- Lestari, R., Bramanto, B., Prijatna, K., Pahlevi, A. M., Putra, W., Muntaha, R. I. S., & Ladivanov, F. (2023). Local geoid modeling in the central part of Java, Indonesia, using terrestrial-based gravity observations. *Geod. Geodyn.*, *14*(3), 231–243. <https://doi.org/10.1016/j.geog.2022.11.007>
- Martinec, Z., Matyska, C., Grafarend, E. W., & Vanicek, P. (1993). On Helmert's 2nd condensation method. *Journal of Geodesy*, *18*(August 2019), 417–421.
- Matsuo, K., & Kuroishi, Y. (2020). Refinement of a gravimetric geoid model for Japan using GOCE and an updated regional gravity field model. *Earth, Planets and Space*, *72*(1). <https://doi.org/10.1186/s40623-020-01158-6>
- Omang, O. C. D., & Forsberg, R. (2000). How to handle topography in practical geoid determination: Three examples. *Journal of Geodesy*, *74*(6), 458–466. <https://doi.org/10.1007/s001900000107>
- Pavlis, N. K., Holmes, S. A., Kenyon, S. C., & Factor, J. K. (2012). The development and evaluation of the Earth Gravitational Model 2008 (EGM2008). *Journal of Geophysical Research: Solid Earth*, *117*(4), 1–38. <https://doi.org/10.1029/2011JB008916>
- Schwarz, K. P., Sideris, M. G., & Forsberg, R. (1987). Orthometric heights without leveling. *J. Surv. Eng.*, *113*(1), 28–40. [https://doi.org/10.1061/\(ASCE\)0733-9453\(1987\)113:1\(28\)](https://doi.org/10.1061/(ASCE)0733-9453(1987)113:1(28))
- Schwarz, K. P., Sideris, M. G., & Forsberg, R. (1990). The Use of FFT Techniques in Physical Geodesy. *Geophys. J. Int.*, *100*, 485–514.
- Sideris, M. G. (2013). Geoid determination by FFT techniques. *Lecture Notes in Earth System Sciences*, *110*, 453–516. https://doi.org/10.1007/978-3-540-74700-0_10
- Sideris, M. G. (2021). *Geoid Determination, Theory and Principles* (H. K. Gupta, Ed.; pp. 476–482). Springer. https://doi.org/10.1007/978-3-030-58631-7_154
- Sideris, M. G., & Forsberg, R. (1991). *Review of Geoid Prediction Methods in Mountainous Regions*. March, 51–62. https://doi.org/10.1007/978-1-4612-3104-2_8
- Sjöberg, L. E. (1984). Least Squares Modification of Stokes and Venning–Meinesz Formulas by Accounting for Errors of Truncation, Potential Coefficients and Gravity Data. In *Technical Report*.
- Sjöberg, L. E. (1991). Refined least squares modification of Stokes' formula. *Journal of Geodesy*, *16*(9), 367–375.
- Sjöberg, L. E. (2003). A general model for modifying Stokes' formula and its least-squares solution. *Journal of Geodesy*, *77*(7), 459–464. <https://doi.org/10.1007/s00190-003-0346-1>
- Sjöberg, L. E. (2020). Unbiased least-squares modification of Stokes' formula. *Journal of Geodesy*, *94*(9), 1–5. <https://doi.org/10.1007/s00190-020-01405-4>
- SRTM. (2015). *The Shuttle Radar Topography Mission (SRTM) Collection User Guide*. 1–17. https://lpdaac.usgs.gov/documents/179/SRTM_User_Guide_V3.pdf

- Tozer, B., Sandwell, D. T., Smith, W. H. F., Olson, C., Beale, J. R., & Wessel, P. (2019). Global Bathymetry and Topography at 15 Arc Sec: SRTM15+. *Earth and Space Science*, 6(10), 1847–1864. <https://doi.org/10.1029/2019EA000658>
- Vanicek, & Kleusberg. (1987). The Canadian geoid - Stokesian approach. *Manusc Geod*, 12, 86–98.
- Vaníček, P., Kingdon, R., Kuhn, M., Ellmann, A., Featherstone, W. E., Santos, M. C., Martinec, Z., Hirt, C., & Avalos-Naranjo, D. (2013). Testing Stokes-Helmert geoid model computation on a synthetic gravity field: Experiences and shortcomings. *Studia Geophys. et Geod.*, 57(3), 369–400. <https://doi.org/10.1007/s11200-012-0270-z>
- Vu, D. T., Bruinsma, S., & Bonvalot, S. (2019). A high-resolution gravimetric quasigeoid model for Vietnam. *Earth, Planets and Space*, 71(1). <https://doi.org/10.1186/s40623-019-1045-3>
- Wang, Y. M., Sánchez, L., Ågren, J., Huang, J., Forsberg, R., Abd-Elmotaal, H. A., Ahlgren, K., Barzaghi, R., Bašić, T., Carrion, D., Claessens, S., Erol, B., Erol, S., Filmer, M., Grigoriadis, V. N., Isik, M. S., Jiang, T., Koç, Ö., Krcmaric, J., ... Zingerle, P. (2021). Colorado geoid computation experiment: overview and summary. *J. Geod.*, 95(12), 127. <https://doi.org/10.1007/s00190-021-01567-9>
- Wong, L., & Gore, R. (1969). Accuracy of Geoid Heights from Modified Stokes Kernels. *Geophysical Journal International*, 18(1), 81–91. <https://doi.org/10.1111/j.1365-246X.1969.tb00264.x>
- Wu, Q., Wang, H., Wang, B., Chen, S., & Li, H. (2020). Performance Comparison of Geoid Refinement between XGM2016 and EGM2008 Based on the KTH and RCR Methods: Jilin Province, China. *Remote Sens.*, 12(2), 324. <https://doi.org/10.3390/rs12020324>
- Yang, M., Hirt, C., & Pail, R. (2020). TGF: A new MATLAB-based software for terrain-related gravity field calculations. *Remote Sensing*, 12(7). <https://doi.org/10.3390/rs12071063>
- Yang, M., Hirt, C., Wu, B., Deng, X. Le, Tsoulis, D., Feng, W., Wang, C. Q., & Zhong, M. (2022). Residual Terrain Modelling: The Harmonic Correction for Geoid Heights. *Surveys in Geophysics*, 43(4), 1201–1231. <https://doi.org/10.1007/s10712-022-09694-4>
- Yildiz, H., Forsberg, R., Ågren, J., Tscherning, C. C., & Sjöberg, L. E. (2012a). Comparison of remove-compute-restore and least squares modification of Stokes' formula techniques to quasi-geoid determination over the Auvergne test area. *J. Geod. Sci.*, 2(1), 53–64. <https://doi.org/10.2478/v10156-011-0024-9>
- Yildiz, H., Forsberg, R., Ågren, J., Tscherning, C., & Sjöberg, L. (2012b). Comparison of remove-compute-restore and least squares modification of Stokes' formula techniques to quasi-geoid determination over the Auvergne test area. *Journal of Geodetic Science*, 2(1), 53–64. <https://doi.org/10.2478/v10156-011-0024-9>
- Zaki, A., & Mogren, S. (2022). A high-resolution gravimetric geoid model for Kingdom of Saudi Arabia. *Survey Review*, 54(386), 375–390. <https://doi.org/10.1080/00396265.2021.1944544>